Effects of UV Irradiation on the Sensing Properties of Co-doped SnO_2 Thin Film for Ethanol Detection

Mikayel Aleksanyan
Department of Physics of Semiconductors and Microelectronics
Yerevan State University
Yerevan, Republic of Armenia
e-mail: maleksanyan@ysu.am

Vladimir Aroutiounian
Department of Physics of Semiconductors and Microelectronics
Yerevan State University
Yerevan, Republic of Armenia
e-mail: kisahar@ysu.am

Artak Sayunts
Department of Physics of Semiconductors and Microelectronics
Yerevan State University
Yerevan, Republic of Armenia
e-mail: sayuntsartak@ysu.am

Valeri Arakelyan
Department of Physics of Semiconductors and Microelectronics
Yerevan State University
Yerevan, Republic of Armenia
e-mail: avaleri@ysu.am

Hayk Zakaryan
Department of Physics of Semiconductors and Microelectronics
Yerevan State University
Yerevan, Republic of Armenia
e-mail: hayk.zakaryan@ysu.am

Gohar Shahnazaryan
Department of Physics of Semiconductors and Microelectronics
Yerevan State University
Yerevan, Republic of Armenia
e-mail: sgohar@ysu.am

Abstract - **In this paper, a sputtering ceramic target based on SnO_2 doped with 2 at.% Co was synthesized by solid-phase reaction method. A chemiresistive alcohol vapor sensor based on SnO_2<Co> was manufactured by the high-frequency magnetron sputtering method. The alcohol sensing properties of the SnO_2<Co> sensor under the ultraviolet (UV) illumination were examined at room temperature (RT). The UV-assisted alcohol sensor showed a sufficient response to low concentrations of alcohol vapor at RT. The Co-doped SnO_2 sensor has also demonstrated a high sensitivity to alcohol vapors at elevated operating temperature. The impedance characteristics of the sensors have been also thoroughly studied. It is expected that in the future, Co doped SnO_2 based sensitive thin films will be able to be utilized in highly sensitive, real-time alcohol vapor sensors.**

Keywords - gas sensor; alcohol; UV radiation; room temperature; metal oxides; Nyquist plot.

I. INTRODUCTION

Today, alcohol vapor sensors have a great demand in various fields. Ethanol sensors are used in the food industry, medicine and biotechnology. Ethanol sensors are also extremely important during the production of ethanol and alcoholic drinks to monitor the beverage quality. They are used in processes such as: food–packaging, clinical analysis, agronomic, vinicultural and veterinary analysis, also toxic waste and contamination analysis, fuel processing, Trends in Analytical Chemistry (TRAC) management and societal applications, as well as chemical processing in industry [1]-[6]. Several methods and strategies have been reported for the detection of ethanol, e.g., gas chromatography, liquid chromatography, refractometry and spectrophotometry, semiconductor gas sensors and so on [3] [7] [8].

The solid-state gas sensors based on Metal Oxide Semiconductors (MOSs) with different nanostructures have played an important role in environmental monitoring, domestic and car safety, control in chemical processing due to their distinct advantages, such as simple implementation, low cost, high sensitivity, stability and reproducibility, low detection limit, easy production, nontoxicity, easy-achieved real-time response and compatibility with micro-fabrication processes [9]-[11]. Various MOSs materials, such as SnO_2, In_2O_3, WO_3, ZnO, TiO_2, Fe_2O_3, CuO, Ga_2O_3, CTO (CrTiO) with different nanostructures and dopant have been studied and showed promising results for detecting Volatile Organic Compounds (VOCs) [12]. Among these materials, the SnO_2 has good electrical and chemical properties. It is an n-type semiconductor with tetragonal rutile structure and it has a large energy band gap of 3.6 eV at 300 K. It has been widely exploited as an ultrasensitive gas sensor for the detection of carbon monoxide (CO), ammonia, ozone, carbon dioxide, hydrogen, hydrogen peroxide, nitrogen dioxide, ethanol and so on [13]-[15]. The wide range of possible applications has attracted many researchers to work on this material with different nanostructures, such as nanograins, nanorods, nanowires and nanofibers synthesized by various methods. It has a high sensitivity to reducing and

oxidizing gases, fast response and recovery behavior and low sensitivity to humidity [16]-[18].

Although many conductometric gas sensors made of MOSs have been commercialized for the last decades, a lot of problems still need to be solved in order to improve the performance of gas sensing devices. The main issues are related to sensitivity, selectivity and stability but the lowering of sensor's operating temperature is still one of the main concerns. Resistive metal oxide based gas sensors normally operate at an elevated temperature (in a range of 200 ºC to 400 ºC). This results in higher power consumption, limits the use of the sensor in explosive environments, and causes difficulties for the sensor to be attached to electrical systems [19] [20].

There are many studies aimed at applying new technologies and reducing operating temperatures. To ensure a low operating temperature, several techniques have been used, such as doping the metal oxides with additives, using catalytic particles, applying a high electric field across the sensor terminals and illuminating the sensors with UV radiation [21] [22]. The irradiation of UV-assisted MOS sensors is an important alternative to activate chemical reactions on the metal oxide surface and reduce the resistance of the thin sensing layer instead of the more common use of energy-demanding heating. Almost completely replacing the effect of thermal energy, UV irradiation greatly influences the adsorption and desorption processes of the gas on the semiconductor surface enhancing their reactivity with the analyte gas. Under the influence of UV illumination, as a result of the formation of electron–hole pairs, more neutral atoms and molecules of absorbed oxygen on the surface of the semiconductor become ions, which then interact with analyte gas. UV irradiation can also be used to clean the active surface of a gas sensing layer, but the more important function is to improve the sensitivity and selectivity of the gas sensor by reducing the operating temperature. If it is not possible to lower the operating temperature to RT by using UV irradiation, UV irradiation combined with heating can be used to stimulate the gas sensor [23]-[25].

In this paper, we focus on low temperature sensing of SnO_2 based thin film sensors under UV illumination. In Section II, the fabrication steps of SnO_2<Co> sensor are presented. In Section III, the studies of sensing properties of UV assisted ethanol sensor are presented. In Section IV, the gas sensing mechanisms are explained. The conclusions are outlined in Section V. The sensor exhibited good sensitivity to low concentration of ethanol vapors. Fabricated sensors have also sufficient selectivity and stability over time.

II. SENSOR FABRICATION

Sensitive layers based on SnO_2<Co> were deposited by the RF magnetron sputtering technique. Firstly, appropriate quantities of the corresponding metal oxide powders (SnO_2+2 at.%Co_2O_3) were weighed and mixed thoroughly for 10 hours. Then, the mixture was subjected to pre-heat treatment at 800 ^{0}C for 5 hours (the initial annealing temperature was chosen based on the composition of the compound). The preheating of mixed powder eliminates the moisture of the metal oxide raw materials, which facilitates homogeneous mixing and milling of the powders (when the ceramic tablet is made of dry powders, it reduces the probability of the formation of mechanical cracks during final annealing). Then, the mixed powder was milled for 20 hours until becoming fully homogeneous and pressed (with 2000 N/cm^2 pressure) in a form of a tablet (with 50 mm diameter). The sputtering ceramic target based on SnO_2 doped with 2 at.% Co (using the pressed tablet) was synthesized by solid-phase reaction method using thermal treatment in the atmosphere by the programmable furnace Nabertherm, HT O4/16 (with the controller of C 42). The final annealing was carried out at temperature range of 500 °C-1100 °C for 20 hours. The synthesized semiconductor solid solution was subjected to mechanical treatment in order to eliminate surface defects. So, a smooth and parallel target with a diameter of 40 mm and thickness of 2 mm was prepared as a magnetron sputtering target (see Figure 1).

The thin sensing layers were deposited on Multi-Sensor-Platforms by the RF magnetron sputtering method using synthesized SnO_2<Co> target. The Multi-Sensor-Platforms were purchased from TESLA BLANTA (Czech Republic). The platform has a temperature sensor (Pt 1000) for controlling the operating temperature. There are platinum heater and interdigitated electrodes on the ceramic substrate of the Multi-Sensor-Platform (see Figure 2). The heater and temperature sensor were covered with an insulating glass layer. Gas sensitive SnO_2<Co> layer was deposited onto the non-passivated electrode structure, so the Multi-Sensor-Platform was converted into a gas sensor. Then, palladium catalytic particles are deposited on the surface of the magnetron sputtered sensing layer the by ion-beam sputtering method for sensitization of the active layer. The working conditions of the high-frequency magnetron sputtering and ion-beam sputtering are presented in Table I (the base pressure was 2×10^4 Pa for both cases). The manufactured sensors were annealed in the air at 350 °C for 4 hours for homogenization of sensing films and stabilizing their parameters. The fabrication steps of photo-assisted gas sensors are presented in Figure 1.

The thickness of the SnO_2<Co> thin film was measured by the Alpha-Step D-300 (KLA Tencor) profiler. The result of the study of the film-substrate transition profile is shown in Figure 3. The thickness of the SnO_2<Co> film was equal to 180 nm.

The electrical and gas sensing properties of the SnO_2<Co> thin layer was measured using a home-made computer-controlled gas testing system. The testing system has a test chamber, pressure sensor (Motorola-MPX5010DP) and a data acquisition system (PCLD-8115) [26]. For measurement of alcohol vapor concentration, the SnO_2<Co> based sensor (the Multi-Sensor-Platform) was attached in the test chamber connecting the six pins (two pins of temperature sensor, two pins of heater and two pins of resistance measurement electrodes, see Figure 2) with the corresponding inputs on sensor holder. The UV LED (λ=365 nm) was attached 0.5 cm away from the active layer with an illumination of 2 mW/cm^2. The gas sensing

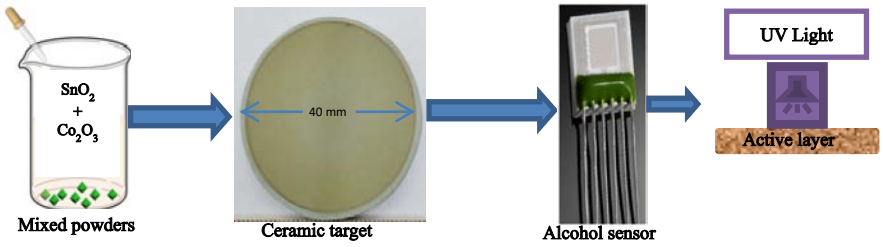

Figure 1. Schematic block diagram of the photo-assisted gas sensor fabrication.

TABLE I. THE WORKING CONDITIONS FOR DEPOSITION OF THIN LAYER AND CATALITIC PARTICLES.

Process	Sputtering duration	Working pressure	Power of generator	Substrate temperature	Cathode current	Anode voltage	Sputtering gas
Magnetron sputtering (RF)	20 m	2×10^{-1} Pa	60 w	200 ^{0}C	---	---	Ar
Ion-beam sputtering (DC)	3 s	5×10^{-1} Pa	---	100 ^{0}C	65 A	25 V	Ar

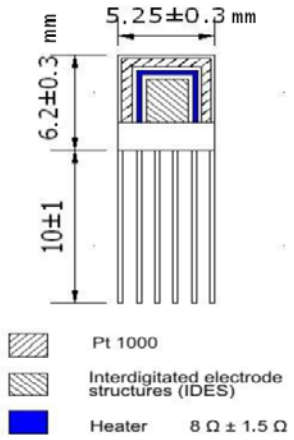

Figure 2. The schematic diagram of the Multi-Sensor-Platform.

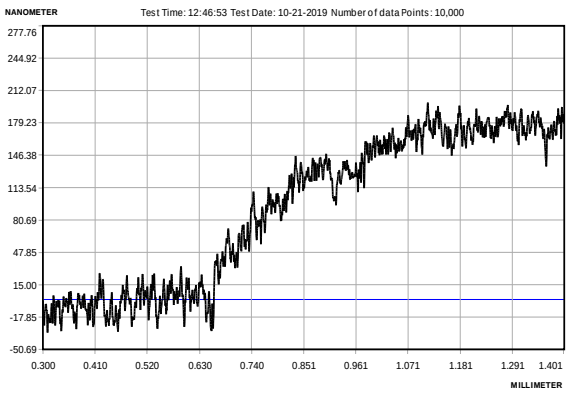

Figure 3. The thickness measurement result for the Co-doped SnO_2 film.

properties of the SnO_2<Co> sensor was measured at RT in the dark and under UV illumination. The response of the sensor was also measured at 200 ^{0}C operating temperature in the dark. The working temperature of the sensor was adjusted by changing the voltage across the platinum heater.

To have the necessary concentration of alcohol vapor in the chamber, the liquid ethanol was introduced into the chamber on the special hot plate designed for the quick conversion of the liquid ethanol to the gas phase. The response of the sensor is defined as $[(R_a-R_g)/R_a]\times100$ %, where R_a and R_g are the electrical resistances of active layer in air and target gas, respectively.

III. GAS SENSING PERFORMANCES

Initially, we tested the influence of the UV illumination on the baseline resistance of the SnO_2<Co> sensor at RT. It can be seen from Figure 4 that the value of R_0/R_{UV} (~350) ratio is larger than 1, indicating the decrease of the sensor baseline resistance under UV illumination.

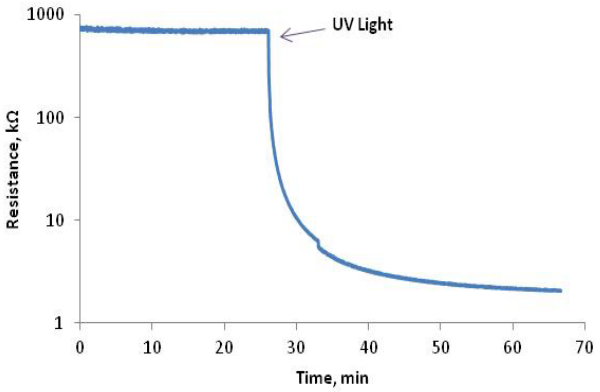

Figure 4. Resistance variation of the Co-doped SnO_2 sensing layer under the influence of UV irradiation at RT.

UV rays generate free carrier in the semiconductor, as a result of which the baseline resistance decreases (These processes are discussed in more detail in Section III). The response time of the Co-doped SnO_2 thin film under UV irradiation is a few minutes.

The manufactured sensor is resistive and its operation is grounded on changes of resistance of gas sensitive semiconductor layer under the influence of ethanol vapors caused by an exchange of charges between molecules of the semiconductor film and absorbed ethanol. The high operating temperature of these types of sensors is mainly due to the high activation energies of chemical reactions. For this reason, these types of sensors are mainly not sensitive at RT. The UV light promotes the gas adsorption and desorption on the surface of the semiconductor participating to the sensing mechanisms [24].

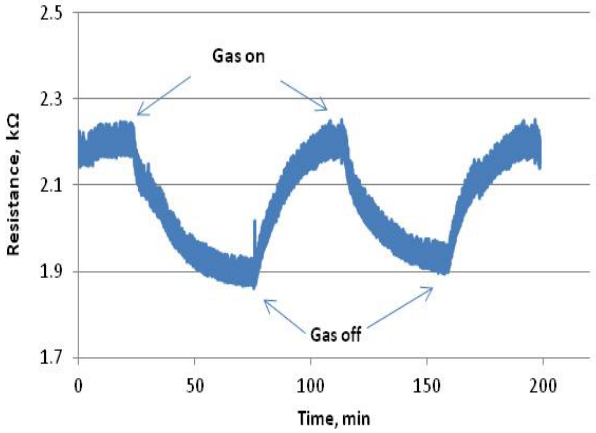

Figure 5. Resistance variation of the SnO_2<Co> sensor under the influence of UV irradiation at RT in the presence of 150 ppm ethanol vapors.

The thin film SnO_2<Co> based sensor did not show sensitivity to ethanol vapors at RT without UV irradiation. We measured the resistance variation (also the signal repeatability) of the SnO_2<Co> sensor in the presence of ethanol vapors under the influence of UV irradiation at RT. The resistance of the thin film changes by almost 400 Ω in the presence of 150 ppm ethanol vapors (see Figure 5).

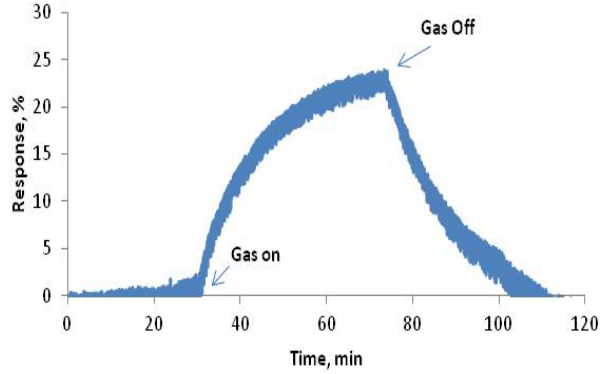

Figure 6. The SnO_2<Co> sensor's response to 900 ppm of ethanol vapors under the influence of UV irradiation at RT.

Sensor response and recovery times are in minutes and it is clear that recovery times are faster because UV light more stimulate the desorption processes from the surface of the sensing layer.

Figure 6 shows the transient response of the SnO_2<Co> sensor in the presence of ethanol vapors under UV light at RT. The response to 900 ppm ethanol vapors under UV illumination is sufficiently high (24 %).

We extracted the response vs. concentration curve for the Co-doped SnO_2 sensitive film. Figure 7 shows the dependence of response on the ethanol vapor concentration under the influence of UV irradiation at RT. The dependence has almost linear characteristic, which will allow not only to detect of ethanol vapors but also to accurately measure the low concentrations of this gas.

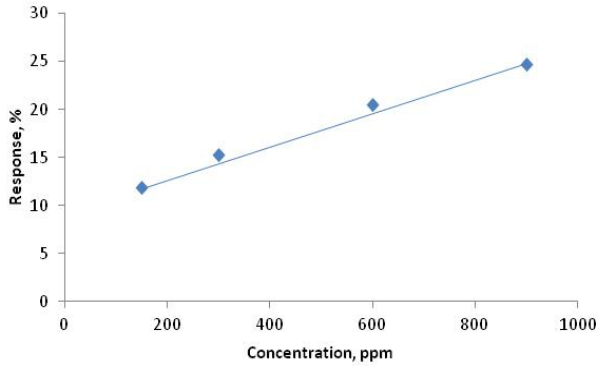

Figure 7. The dependence of response on the ethanol vapor concentration under the influence of UV irradiation at RT.

The gas sensing properties of the Co-doped SnO_2 sensor under the influence of ethanol vapors in dark conditions at high operating temperatures and under the influence of UV irradiation combined with heating were also studied. The sensor's responses to ethanol vapors at different operating temperatures were initially measured with UV irradiation.

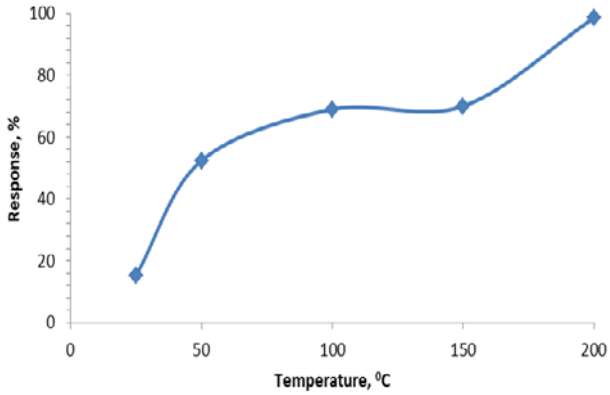

Figure 8. The dependence of response on the operating temperature of the SnO_2<Co> sensor under the influence of UV irradiation at the presence of 300 ppm ethanol vapors.

Figure 8 shows the dependence of response on the operating temperature of the SnO_2<Co> sensor under the influence of UV irradiation at the presence of 300 ppm ethanol vapors. As expected, in the case of not very high operating temperatures (up to 200 ^{0}C), the increase in temperature is accompanied by an increase in the response,

because the chemical reactions at higher operating temperatures are faster and more efficient.

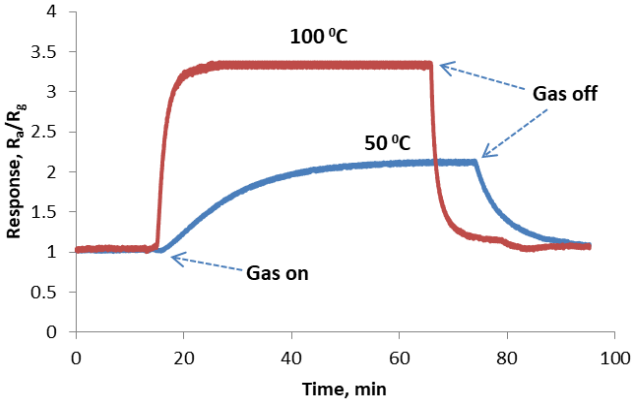

Figure 9. The SnO_2<Co> sensor's responses to 300 ppm of ethanol vapors under the influence of UV irradiation at different operating temperature.

The sensor's responses were also compared at different operating temperatures under the influence of UV irradiation in dark conditions. It should be noted that the sensor did not show sensitivity to alcohol vapors at 50 ^{0}C and 100 ^{0}C operating temperatures in dark conditions. The SnO_2<Co> sensor's responses to 300 ppm of ethanol vapors under the influence of UV irradiation at 50 ^{0}C and 100 ^{0}C operating temperatures are presented in Figure 9 (At high operating temperatures, as we are dealing with higher response values, it is desirable to use an absolute response definition: R_a/R_g). The effect of the UV irradiation at these temperatures gave the sensor increased sensitivity and as expected, at 100 ^{0}C we had a higher response and shorter recovery and response times.

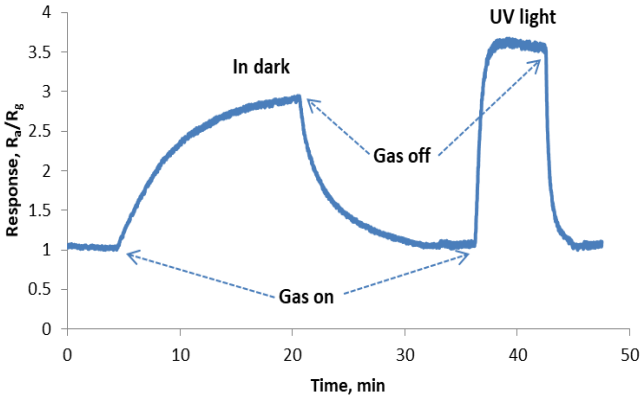

Figure 10. The SnO_2<Co> sensor's responses to 300 ppm of ethanol vapors at 150 ^{0}C operating temperature in dark conditions and under the influence of UV irradiation.

The SnO_2<Co> sensor's responses to 300 ppm of ethanol vapors at 150 ^{0}C operating temperature in dark conditions and under the influence of UV irradiation are presented in Figure 10. The effect of the UV irradiation dramatically improves the speed and the response of the sensor.

Since the maximum response in the observed operating temperature range (25-200 ^{0}C) was recorded at 200 ^{0}C operating temperature, the gas sensitivity characteristics of the sensor were studied in more detail at this temperature. The sensitive layer's resistance decreases more than 25 times in the presence of 150 ppm ethanol vapors at 200 ^{0}C operating temperature (see Figure 11). The response and recovery times of the sensor at high operating temperatures are a few seconds.

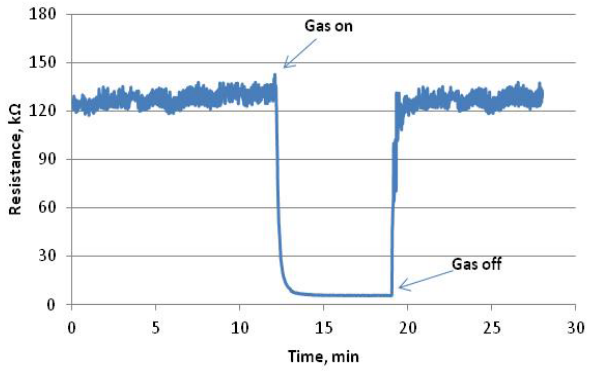

Figure 11. Resistance variation of the SnO_2<Co> sensor in the presence of 150 ppm ethanol vapors at 200 °C operating temperature in dark conditions.

The sensor showed sensitivity (R_a/R_g=3) to the extremely low concentrations (0.5 ppm) of ethanol vapors at 200 ^{0}C operating temperature even in dark conditions. The presence of the UV irradiation increases the response to 3.5 and reduces the recovery time (see Figure 12).

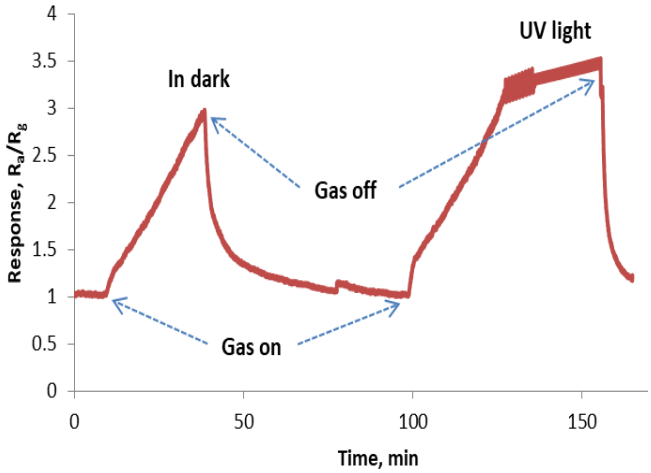

Figure 12. The SnO_2<Co> sensor's responses to 0.5 ppm of ethanol vapors at 200 ^{0}C operating temperature in dark condition and under the influence of UV irradiation.

Figure 13 shows the SnO_2<Co> sensor's responses to different concentrations of ethanol vapors at 200 ^{0}C operating temperature under the influence of UV irradiation. The sensor's response to 300 ppm ethanol vapors is 75, which is extremely high. The response and recovery times

of the sensor at 200 ^{0}C operating temperature are a few seconds at relatively high concentrations (300 ppm and 100 ppm) but, as the concentration decreases, the response times increase. It is assumed that, in the case of low concentrations, the saturation of the gas-sensitive surface with ethanol molecules occurs delayed, which leads to an increase in the response time of the sensor.

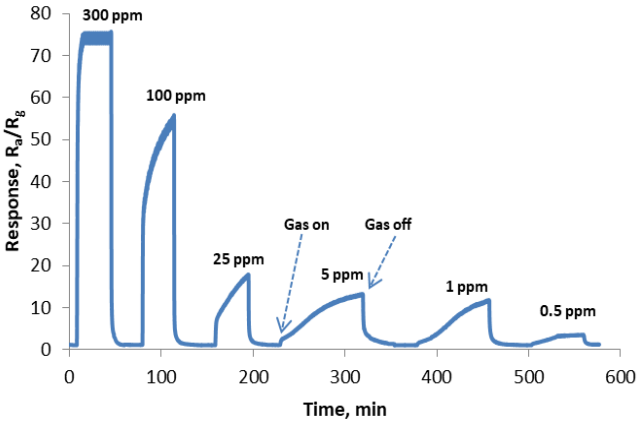

Figure 13. The SnO_2<Co> sensor's responses to different concentrations of ethanol vapor at 200 ^{0}C operating temperature under the influence of UV irradiation.

The response vs. concentration curve of the sensor was also extracted under the influence of UV irradiation at 200 ^{0}C operating temperature (Figure 14). The dependence has almost linear characteristic at the concentration range of 0.5 to 100 ppm, but in the case of higher concentration, we have a deviation from the initial linear curve. At higher concentration, the angle of the linear curve changes and it is expected, that it will also be linear (which will show our future experimental work).

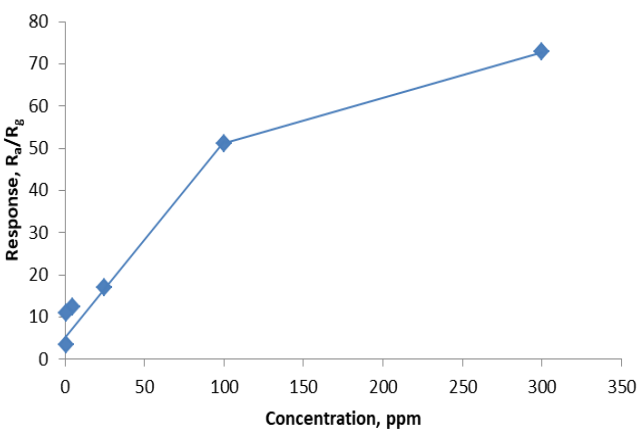

Figure 14. The dependence of response on the ethanol vapor concentration under the influence of UV irradiation at 200 °C operating temperature.

So, if it is not possible to lower the operating temperature to RT by using UV irradiation, UV irradiation combined with heating can be used to stimulate the gas sensor. At high operating temperature both in dark conditions and with UV irradiation, the sensor performance is quite promising but the power consumption of fabricated sensor at 200 ^{0}C is about 2.5 W. It is more than two orders high then the power consumption (24 mW) needed the sensor operating with UV irradiation at RT.

The alcohol responses of the SnO_2<Co> based sensor were also compared with those described in previous reports (Table II). Our UV-activated SnO_2<Co> based sensor exhibits much lower working temperature and comparable ethanol response compared with the previously reported ethanol sensors with and without UV illumination. Our UV activated SnO_2<Co> sensor displays better ethanol response to extremely low concentration (0.5 ppm) of ethanol than most of the reported oxide-based sensors under UV irradiation.

TABLE II. THE COMPARISON OF ETHANOL VAPOR SENSOR RESPONSE BETWEEN THIS WORK AND PREVIOUSLY PUBLISHED REPORTS.

Sensing materials	Conc. (ppm)	Temp. (^{0}C)	Resp.	UV light	Ref.
SnO_2-Zn_2SnO_4	200	300	5	No	[27]
ZnO	150	53	1.7	Yes	[28]
Zn_2SnO_4	200	130	32.5	Yes	[29]
ZnO:AuNPs	1000	125	6.3	Yes	[30]
SnO_2-ZnO	100	160	1.1	No	[31]
SnO_2-GaN	500	RT	1.01	Yes	[32]
NiO	500	200	4.94	Yes	[33]
SnO_2	300	240	65	Yes	[34]
SnO_2<Co>	900	RT	1.4	Yes	This work
SnO_2<Co>	0.5	200	5	Yes	This work

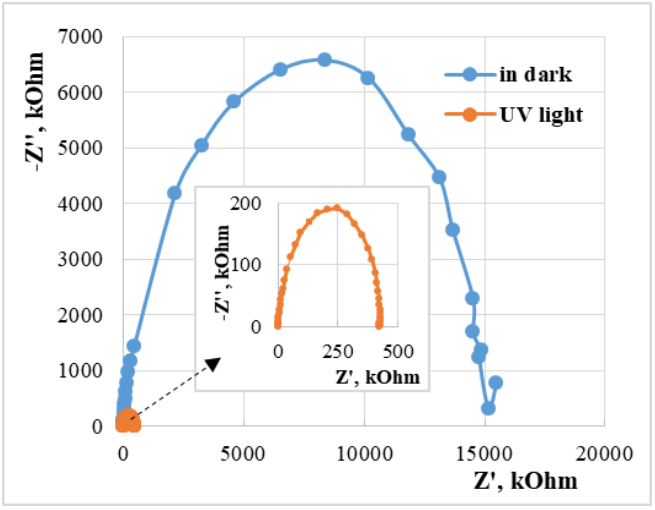

Figure 15. The Nyquist plots of SnO_2<Co> sensor observed under dark condition and in the presence of UV irradiation at RT.

There were also studied the gas sensing properties of the Co-doped SnO_2 sensor by impedance spectroscopy using the ZIVE-SP1 Potentiostat and the Keithley 4200-SCS (Semiconductor Characterization System) under the influence of ethanol vapors in dark conditions at high operating temperatures and under the influence of UV irradiation combined with heating.

Figure 15 shows the Nyquist plots of SnO_2<Co> sensor observed under dark condition and in the presence of UV irradiation at RT. The UV response is quite large presented by the deviation of the semicircular Nyquist plots.

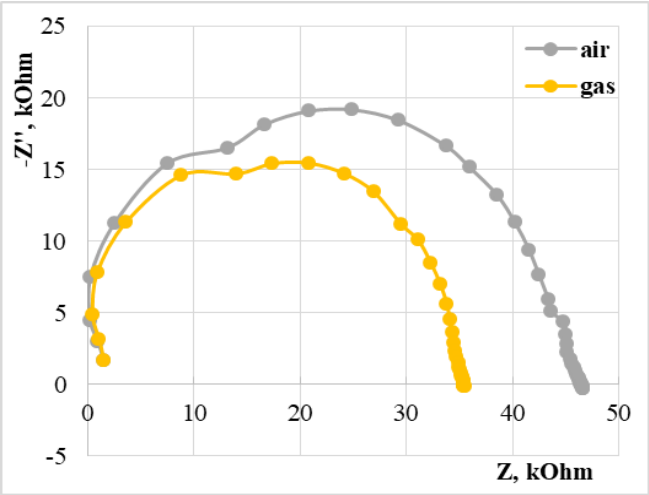

Figure 16. The Nyquist plots of SnO_2<Co> sensor observed in the air and in the presence of 300 ppm ethanol vapors at 50 ^{0}C operating temperature under the influence of UV irradiation.

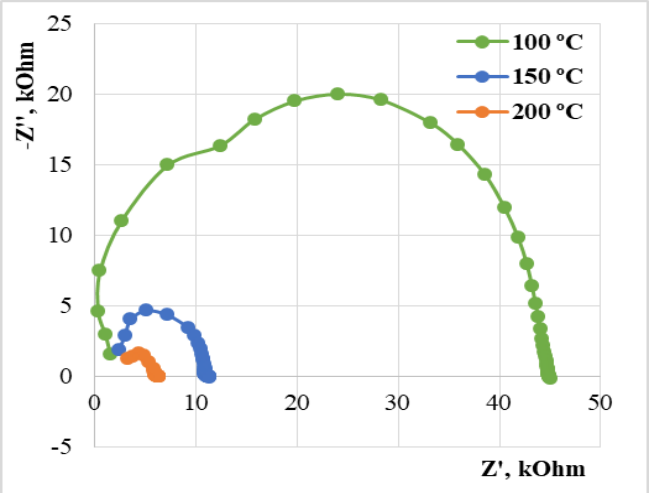

Figure 17. The Nyquist plots of SnO_2<Co> sensor observed in the presence of 300 ppm ethanol vapors at different operating temperatures without UV irradiation.

The sensor did not show sensitivity to alcohol vapors at 50 ^{0}C in dark conditions, but at this operating temperature under the influence of UV irradiation the response was significant. The Nyquist plots of the sensor observed in the air and in the presence of 300 ppm ethanol vapors at 50 ^{0}C operating temperature under the influence of UV irradiation are presented in Figure 16. The significant deviation of Nyquist plots at the presence of ethanol vapors was observed.

The Nyquist plots of SnO_2<Co> sensor observed in the presence of 300 ppm ethanol vapors at different operating temperatures under the influence of UV irradiation and in the dark condition are presented in Figure 17 and Figure 18. The semicircle plots were obtained for Nyquist impedance, which indicates that the diameter of the semicircles increased gradually when the temperature was decreased. It is assumed that the deviation of the semicircles from the zero point by the influence of UV irradiation is related to the direct effect of the UV-activated adsorption/desorption processes on the impedance properties.

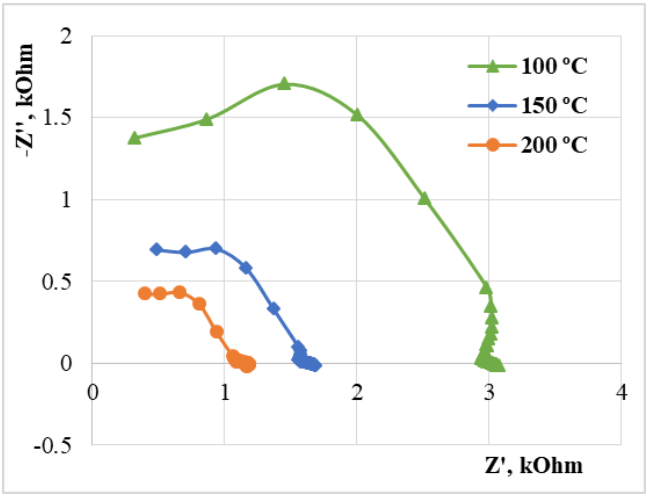

Figure 18. The Nyquist plots of SnO_2<Co> sensor observed in the presence of 300 ppm ethanol vapors at different operating temperatures under the influence of UV irradiation.

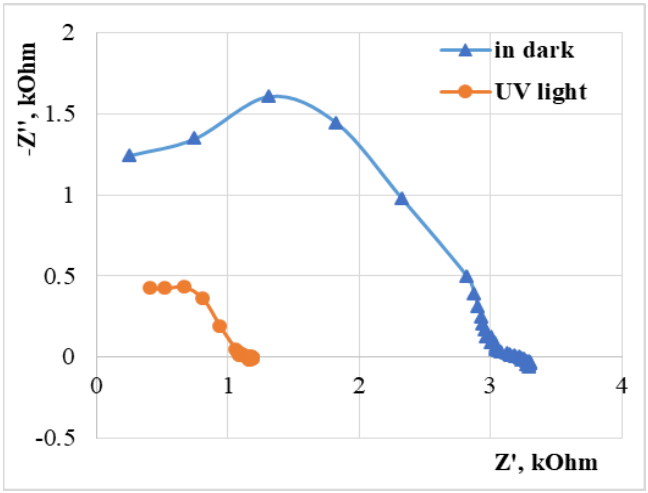

Figure 19. The Nyquist plots of SnO_2<Co> sensor observed in the presence of 300 ppm ethanol vapors at 200 ^{0}C operating temperature under dark condition and in the presence of UV irradiation.

Figure 19 shows that Nyquist impedance of SnO_2<Co> sensor recorded in the presence of 300 ppm ethanol vapors at 200 ^{0}C operating temperature under dark condition and in the presence of UV irradiation. The impact of the UV irradiation dramatically reduced the diameter of the semicircle by shifting the curve to lower ranges of the resistance. This is due to the change of the localized charges and free carriers concentration on the active surface of the semiconductor.

The frequency dependencies for the real and imaginary components of the impedance for the SnO_2<Co> sensor were also extracted (see Figure 20 and Figure 21). The deflection of the curves under the influence of UV light in the case of the imaginary components of the impedance depends more on the frequency. It is clear from the Figure 21 that the deviation is more significant in the case of high frequencies. This is due to the fact that at high frequencies the capacitive properties of the sensitive film are revealed.

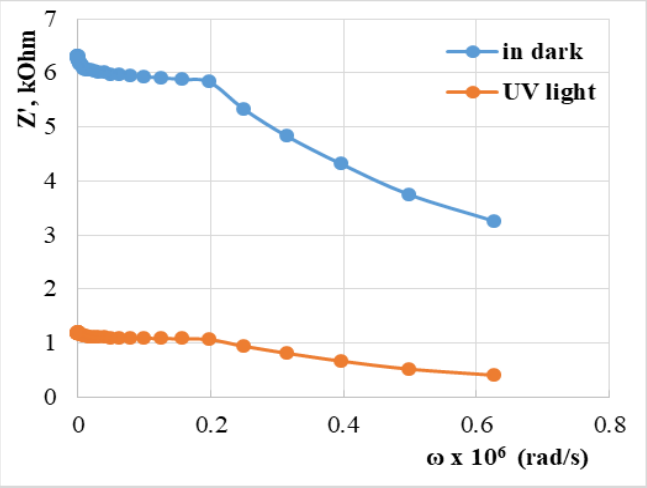

Figure 20. Frequency dependencies for the real component of the impedance for the SnO_2<Co> in the presence of 300 ppm ethanol vapors at 200 ^{0}C operating temperature under dark condition and in the presence of UV irradiation.

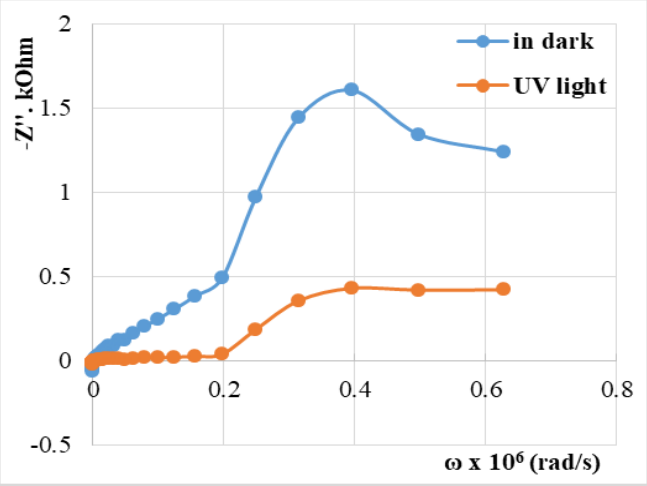

Figure 21. Frequency dependencies for the imaginary component of the impedance for the SnO_2<Co> in the presence of 300 ppm ethanol vapors at 200 ^{0}C operating temperature under dark condition and in the presence of UV irradiation.

Our future researches will focus not only on the study of the deviations of Nyquist plots of the SnO_2<Co> sensor at the presence of ethanol vapors under the influence of UV irradiation, but also on the build of the sensor equivalent circuit, obtaining more comprehensive information about the gas-sensitive element.

The sensor's responses to acetone and toluene vapors were also measured. The sensor showed negligible sensitivity to acetone vapors, but did not show any sensitivity to toluene vapors, thus, the sensor has a high selectivity in the presence of VOCs.

The fabricated sensors can be also easily attached to modern Arduino systems for data extraction and evaluation.

IV. GAS SENSING MECHANISM

To explain the observed sensing behavior of the Co-doped SnO_2 sensor, the gas sensing mechanism under dark and UV light conditions has to be taken into account. The basis of the operation of conductometric sensors is the change in resistance under the effect of reactions taking place on the surface of the sensing layer [35]-[37]. The target gases (chemical species) interact with the sensitive layer and thus modulate its electrical conductance. The gas sensing mechanism includes consideration of the role of the chemisorbed oxygen. The initial exposure to air results in oxygen adsorption on the surface through transferring electrons from the conduction band to the adsorbed oxygen. The oxygen chemisorption means the formation of O^{2-}, O^- and O_2^- species on the surface. They originate due to electrons which are captured by adsorbed neutral oxygen species on the surface of the oxide. For the n-type semiconductor the majority charge carriers are electrons and upon interaction with a reducing gas an increase in conductivity occurs [38]-[40]. The oxygen ions are adsorbed mainly molecularly (O_2^-) in the absence of UV radiation and atomic oxygen ions (O^- and O^{2-}) may be formed on the surface of the illuminated sensor, as shown in the following reactions [24] [41]:

$$O_{2\,(gas)} \leftrightarrow O_{2\,(adsorbed)} \quad (1)$$

$$O_{2\,(adsorbed)} + e^-_{(hv)} \leftrightarrow O^-_{2\,(adsorbed)} \quad (2)$$

$$O_{2(gas)} + e^-_{(hv)} \leftrightarrow O^-_{2\,(adsorbed)} \quad (3)$$

$$O^-_{2\,(adsorbed)} + e^-_{(hv)} \leftrightarrow 2O^-_{(adsorbed)} \quad (4)$$

$$O^-_{(adsorbed)} + e^-_{(hv)} \leftrightarrow O^{2-}_{(adsorbed)} \quad (5)$$

UV illumination changes the number of charge carriers on the surface of the film through exciting electrons from the material valence band to the conduction band, which results in a decrease in sensor resistance and an increase of the number of surface atomic oxygen ions. The oxygen chemisorption results in a modification of the space charge region toward depletion.

Upon exposure to alcohol vapors, the ethanol molecules react with surface oxygen species and produce electrons, resulting in an increase of electrical conductance of the n-type semiconductor (Co-doped SnO_2 sensitive film). The appropriate reactions are expressed as follows [42]-[44]:

$6O^-_{(adsorbed)} + C_2H_5OH_{(gas)} \rightarrow 3H_2O_{(gas)} + 2CO_{2\ (gas)} + 6e^-$ (6)

$3O_2^-{}_{(adsorbed)} + C_2H_5OH_{(gas)} \rightarrow 3H_2O_{(gas)} + 2CO_{2(gas)} + 3e^-$ (7)

$6O^{2-}{}_{(adsorbed)} + C_2H_5OH_{(gas)} \rightarrow 3H_2O_{(gas)} + 2CO_{2(gas)} + 12e^-$ (8)

The continuous UV illumination promotes the formation of more atomic oxygen ions (O^- and O^{2-}) on the surface of the semiconductor, which leads to increased sensitivity.

V. CONCLUSION

In summary, a simple technology has been used to manufacture semiconductor thin film sensor based on SnO_2 doped with 2 at.% Co. The fabricated SnO_2<Co> chemiresistive gas sensor showed a good sensitivity to different concentrations of ethanol vapor (from 150 to 900 ppm) at RT with the activation of low-powered UV LED (24 mW, 365 nm). The sensor also showed sensitivity to extremely low concentrations (0.5 ppm) of ethanol vapors at 200 ^{0}C operating temperature even in dark condition and the presence of the UV irradiation increases the response and reduces the recovery time. The sensor displayed a good signal repeatability and long-term stability. The sensor provides not only high response to ppm level of alcohol vapors but also significant deviation of Nyquist plots at the presence of alcohol vapors. These sensing characteristics made the present SnO_2<Co> based sensor a promising candidate for practically detecting ethanol vapors at the temperature range of 25 to 200 ^{0}C.

ACKNOWLEDGMENT

This investigation was supported by 19YR-2K002 (Young Researchers 2019-2021) project of Ministry of Education, Science, Culture and Sport RA (Science Committee).

REFERENCES

[1] M. Aleksanyan, A. Sayunts, H. Zakaryan, V. Aroutiounian, V. Arakelyan, and G. Shahnazaryan, "UV-assisted Chemiresistive Alcohol Sensor Based on Cobalt Doped Tin Dioxide," The Fifth International Conference on Advances in Sensors, Actuators, Metering and Sensing (ALLSENSORS 2020) IARIA, Nov. 2020, pp. 1-9, ISBN 978-1-61208-766-5.

[2] M. A. Lakhanea, A. L. Choudharia, R. S. Khairnara, and M. P. Mahabolea, "Alcohol Sensor Based on Mg-STI zeolite Thick Films," Procedia Technology, vol. 24, pp. 595-602, 2016.

[3] A. Charishma, A. Jayarama, V. V. D. Shastrimath, and R. Pinto, "An Ethanol Sensor Review: Materials, Techniques and Performance," SAHYADRI International Journal of Research, vol. l 3, pp. 37-46, June 2017.

[4] E. C. Ramaa et al., "Comparative study of different alcohol sensors based on Screen-Printed Carbon Electrodes," Analytica Chimica Acta, vol. 728, pp. 69-76, 2012, doi:10.1016/j.aca.2012.03.039.

[5] Y. Li et al., "In situ decoration of Zn_2SnO_4 nanoparticles on reduced graphene oxide for high performance ethanol sensor," Ceramics International, vol. 44, pp. 6836–6842, January 2018, doi:org/10.1016/j.ceramint.2018.01.107.

[6] Z. Qin et al., "Highly sensitive alcohol sensor based on a single Er-doped In_2O_3 nanoribbon," Chemical Physics Letters, vol. 646, pp. 12–17, 2016, doi:10.1016/j.cplett.2015.12.054.

[7] G. Feng, M. Zhang, S. Wang, C. Song, and J. Xiao, "Ultra-fast responding and recovering ethanol sensors based on CdS nanospheres doped with graphene," Applied Surface Science, vol. 453, pp. 513–519, May 2018, doi:10.1016/j.apsusc.2018.05.102.

[8] M. Shashikant, V. Lahade1, Mr. Pravin, and D. Pardhi, "Gas Sensing Technologies: Review, Scope and Challenges," International Journal of Recent Trends in Engineering & Research (IJRTER), vol. 04, pp. 108-115, February 2018, doi: 10.23883/IJRTER.2018.4073.M2XNS.

[9] Y. Shen et al., "Highly sensitive and selective room temperature alcohol gas sensors based on TeO_2 nanowires," Journal of Alloys and Compounds, vol. 664, pp. 229-234, 2016, doi: 10.1016/j.jallcom.2015.12.247.

[10] V. M. Aroutiounian et al., "Manufacturing and investigations of i-butane sensor made of SnO_2/multiwall-carbon-nanotube nanocomposite," Sensors and Actuators B, vol. 173, pp. 890-896, 2012, doi:10.1016/j.snb.2012.04.039.

[11] V. M. Arakelyan et al., "Gas sensors made of multiwall carbon nanotubes modified by tin dioxide," Journal of Contemporary Physics (Armenian Academy of Sciences), vol. 48, pp. 176-183, 2013, doi:10.3103/S1068337213040063.

[12] G. Korotcenkov and B. K. Cho, "Metal oxide composites in conductometric gas sensors: Achievements and challenges," Sensors and Actuators B, vol. 244, pp. 182-210, June 2017, doi:10.1016/j.snb.2016.12.117.

[13] V. Aroutiounian et al., "Thin-film SnO_2 and ZnO detectors of hydrogen peroxide vapors," Journal of Sensors and Sensor Systems, vol. 7, pp. 281-288, April 2018, doi: /10.5194/jsss-7-281-2018.

[14] H. S. Jeong, M. J. Park, S. H. Kwon, H. J. Joo, S. H. Song, and H. I. Kwon, "Low temperature NO_2 sensing properties of RF-sputtered SnO-SnO_2 heterojunction thin-film with p-type semiconducting behavior," Ceramics International, vol. 44, pp. 17283–17289, June 2018, doi:10.1016/j.ceramint.2018.06.189.

[15] V. Aroutiounian et al., "Nanostructured sensors for detection of hydrogen peroxide vapours," Sensors & Transducers, vol. 213, pp. 46-53, June 2017.

[16] G. Korotcenkov and V. Nehasil, "The role of Rh dispersion in gas sensing effects observed in SnO_2 thin films," Materials Chemistry and Physics, vol. 232, pp. 160-168, June 2019, doi:10.1016/j.matchemphys.2019.04.069.

[17] G. Korotcenkov and B. K. Cho, "Thin film SnO_2-based gas sensors: Film thickness influence," Sensors and Actuators B, vol. 142, pp. 321-330, October 2009, doi:10.1016/j.snb.2009.08.006.

[18] M. S. Aleksanyan, "Methane sensor based on $SnO_2/In_2O_3/TiO_2$ nanostructure," Journal of Contemporary Physics (Armenian Academy of Sciences), vol. 45, pp. 77-80, 2010, doi:10.3103/S1068337210020052.

[19] N. Li, Y. Fan, Y. Shi, Q. Xiang, X. Wang, and J. Xu, "A low temperature formaldehyde gas sensor based on hierarchical SnO/SnO_2 nano-flowers assembled from ultrathin nanosheets: Synthesis, sensing performance and mechanism," Sensors and Actuators B, vol. 294, pp. 106-115, September 2019, doi:10.1016/j.snb.2019.04.061.

[20] I. Kortidis, H. C. Swart, S. S. Ray, and D. E. Motaung, "Detailed understanding on the relation of various pH and synthesis reaction times towards a prominent low temperature H_2S gas sensor based on ZnO nanoplatelets," Result in Physics, vol. 12, pp. 2189-2201, March 2019, doi:10.1016/j.rinp.2019.01.089.

[21] E. Espid, A. S. Noce, and F. Taghipour, "The effect of radiation parameters on the performance of photo-activated gas sensors," Journal of Photochemistry & Photobiology A, vol. 374, pp. 95–105, January 2019, doi:10.1016/j.jphotochem.2019.01.038.

[22] J. Cui, L. Shi, T. Xiea, D. Wang, and Y. Lin, "UV-light illumination room temperature HCHO gas-sensing mechanism of ZnO with different nanostructures," Sensors and Actuators B, vol. 227, pp. 220–226, 2016, doi:10.1016/j.snb.2015.12.010.

[23] E. Espid and F. Taghipour, "Development of highly sensitive ZnO/In_2O_3 composite gas sensor activated by UV-LED," Sensors and Actuators B, vol. 241, pp. 828–839, 2017, doi:10.1016/j.snb.2016.10.129.

[24] B. Gong et al., "UV irradiation-assisted ethanol detection operated by the gas sensorbased on ZnO nanowires/optical fiber hybrid structure," Sensors and Actuators B, vol. 245, pp. 821–827, 2017, doi:10.1016/j.snb.2017.01.187.

[25] A. Ilina et al., "UV effect on NO_2 sensing properties of nanocrystalline In_2O_3," Sensors and Actuators B, vol. 231, pp. 491–496, 2016, doi:10.1016/j.snb.2016.03.051.

[26] Z. Adamyan et al., "Nanocomposite sensors of propylene glycol, dimethylformamide and formaldehyde vapors," J. Sens. Sens. Syst., vol. 7, pp. 31-41, 2018, doi:10.5194/jsss-7-31-2018.

[27] C. Chen, G. Z. Li, J. H. Li, and Y. L. Liu, "One-step synthesis of 3D flower-like Zn_2SnO_4 hierarchical nanostructures and their gas sensing properties," Ceramics International, vol. 41, pp. 1857-1862, 2015, doi: 10.1016/j.ceramint.2014.09.136.

[28] C. H. Lin, S. J. Chang, W. S. Chen, and T. J. Hsueh, "Transparent ZnO-nanowire-based device for UV light detection and ethanol gas sensing on c-Si solar cell," RSC Advances, vol. 6, pp. 11146-11150, 2016.

[29] X. Xin et al., "UV-activated porous Zn_2SnO_4 nanofibers for selective ethanol sensing at low temperatures," Journal of Alloys and Compounds, vol. 780, pp. 228-236, 2019, doi: 10.1016/j.jallcom.2018.11.320.

[30] E. Wongrat, N. Chanlek, C. Chueaiarrom, B. Samransuksamer, N. Hongsith, and S. Choopun, "Low temperature ethanol response enhancement of ZnO nanostructures sensor decorated with gold nanoparticles exposed to UV illumination," Sensors and Actuators A, vol. 251, pp. 188–197, 2016, doi: 10.1016/j.sna.2016.10.022.

[31] S. H. Yan et al., "Synthesis of SnO_2-ZnO heterostructured nanofibers for enhanced ethanol gas-sensing performance," Sensors and Actuators B, vol. 221, 88–95, 2015, doi: 10.1016/j.snb.2015.06.104.

[32] R. Bajpai et al., "UV-assisted alcohol sensing using SnO_2 functionalized GaN nanowire devices," Sensors and Actuators B, vol. 171-172, pp. 499–507, 2012, doi: 10.1016/j.snb.2012.05.018.

[33] C. Zhao, J. Fu, Z. Zhang, and E. Xie, "Enhanced ethanol sensing performance of porous ultrathin NiO nanosheets with neck-connected networks," RSC Advances, vol. 3, pp. 4018–4023, 2013.

[34] L. Xu, W. Zeng, and Y. Li, "Synthesis of morphology and size-controllable SnO_2 hierarchical structures and their gas-sensing performance," Applied Surface Science, vol. 457, pp. 1064–1071, 2018, doi: 10.1016/j.apsusc.2018.07.018.

[35] C. Wang, L. Yin, L. Zhang, D. Xiang, and R. Gao, "Metal oxide gas sensors: sensitivity and influencing factors," Sensors, vol. 10, pp. 2088-2106, 2010, doi: 10.3390/s100302088.

[36] C. Zhang, G. Liu, X. Geng, K. Wu, and M. Debliquy, "Metal oxide semiconductors with highly concentrated oxygen vacancies for gas sensing materials: A review," Sensors and Actuators A, vol. 309, pp. 112026, July 2020, doi: 10.1016/j.sna.2020.112026.

[37] V. Brinzari and G. Korotcenkov, "Kinetic approach to receptor function in chemiresistive gas sensor modeling of tin dioxide. Steady state consideration," Sensors and Actuators B, vol. 259, pp. 443-454, April 2018, doi: 10.1016/j.snb.2017.12.023.

[38] R. Arora, U. Mandal, P. Sharma, and A. Srivastav, "Nano composite film Based on Conducting Polymer, SnO_2 and PVA," Materials Today: Proceedings, vol. 4, pp. 2733-2738, 2017, doi: 10.1016/j.matpr.2017.02.150.

[39] M. S. Aleksanyan, V. M. Arakelyan, V. M. Aroutiounian, and G. E. Shahnazaryan, "Investigation of Gas Sensor Made of In_2O_3:Ga_2O_3 Film," Journal of Contemporary Physics (Armenian Academy of Sciences), vol. 46, pp. 86-92, February 2011, doi: 10.3103/S1068337211020071.

[40] S. Zhanga, T. Lei, D. Li, G. Zhang, and C. Xie, "UV light activation of TiO_2 for sensing formaldehyde: How to be sensitive, recovering fast, and humidity less sensitive," Sensors and Actuators B, vol. 202, pp. 964–970, June 2014, doi: 10.1016/j.snb.2014.06.063.

[41] V. M. Arakelyan et al., "Gas sensors made of multiwall carbon nanotubes modified by tin dioxide," Journal of Contemporary Physics (Armenian Academy of Sciences), vol. 48, pp. 176-183, June 2013, doi: 10.3103/S1068337213040063.

[42] Z. Qina et al., "Highly sensitive alcohol sensor based on a single Er-doped In_2O_3 nanoribbon," Chemical Physics Letters, vol. 646, pp. 12-17, 2016, doi: 10.1007/s11664-008-0596.

[43] G. Feng, M. Zhang, S. Wang, C., Song, and J. Xiao, "Ultra-fast responding and recovering ethanol sensors based on CdS nanospheres doped with grapheme," Applied Surface Science, vol. 453, pp. 513-519, September 2018, doi: 10.1016/j.apsusc.2018.05.102.

[44] M. Aleksanyan, "Solid-State Sensors for Ethanol Detection," International Journal of Engineering and Artificial Intelligence (IJEAI), vol. 1, pp. 30-43, 2020.